Investigation of effects of long-term thermal aging on magnetization process in low-alloy pressure vessel steels using first-order-reversal-curves

Satoru Kobayashi, $^{1, a)}$ Ferenc Gillemot, 2 Ákos Horváth, 2 Márta Horváth, 2 László Almásy, 3 Qiang Tian, 4 and Artem Feoktystov 5

(Dated: 17 October 2016)

We have investigated effects of long-term thermal aging at 550°C up to 10000 h on major-loop coercivity, hysteresis scaling of minor loops, and first-order reversal curves (FORCs) for low-alloy pressure vessel steels with low and high Ni contents. While major-loop coercivity and minor-loop coefficient of the scaling exhibit a gradual decrease with aging for high-Ni steel, those for low-Ni one are very weakly dependent on aging time. On the other hand, we found that FORC distribution becomes steep along both axes of interaction and switching fields and the peak shifts toward a lower switching field for both steels. Considering that there is no significant development of nanoscale precipitates during the aging as revealed with small-angle neutron scattering experiments, a relaxation of lattice strain in a matrix, possibly associated with diffusion of Ni atoms, may dominate magnetic properties at 550°C.

I. INTRODUCTION

A development of nondestructive evaluation techniques including a magnetic method for irradiation hardening in reactor pressure vessel steels is an important issue for long-term operation of nuclear power plants. During operation, the steels are exposed to neutron irradiation and high temperatures of 290°C, resulting in the formation of nanoscale defects^{1,2}. Recent magnetic investigations revealed a change of magnetic hysteresis during neutron irradiation, however, the detailed mechanism was not fully understood, primarily due to combined effects of irradiation effects (defect formation) and thermal embrittlement (recovery)^{3–5}. Investigations of steels subjected to thermal aging may give an insight into thermal embrittlement, and therefore into irradiation effect by comparing data for aged and irradiated steels.

We here investigate an effect of long-term thermal aging on magnetic hysteresis for VVER440 and high-Ni VVER1000 low-alloy pressure vessel steels. In addition to hysteresis scaling method using symmetrical minor loops, that we extensively investigated due to its low measurement field useful for a possible application to nondestructive evaluation technique^{6,7}, we also focused on first-order reversal curves (FORCs); they are one kind of asymmetrical minor loops and give several information on domain-wall pinning such as switching field distribution, irreversible and reversible magnetization^{8,9}.

TABLE I. Chemical compositions of the measured alloys (wt.%)

Alloy	Cu	Ni	Mn	Cr	Мо	Fe
VVER440	0.09	0.07	0.54	2.70	0.68	Bal.
VVER1000	0.07	1.26	0.46	2.20	0.50	Bal.

II. EXPERIMENTAL PROCEDURE

We focus on two Russian-type reactor pressure vessel steels VVER440 and VVER1000, with different Ni content; their chemical compositions are listed in Table 1. Blocks of the steels were aged at a high temperature of 550° C up to 10 kh to accelerate thermal effects. After aging, plate samples with dimensions of $4\times16\times0.5~\mathrm{mm}^3$ were cut from the block sample. For each aging condition, 1-6 plate samples were prepared. The change of magnetic properties was surveyed with two different analysis methods; hysteresis scaling of symmetrical minor loops and FORC diagram.

For the analysis of the hysteresis scaling, a set of symmetrical minor B-H loops with different field amplitudes, $H_{\rm a}$, up to 9 kA/m was measured with a field sweep rate of 9 kA/m/s, using a flux meter designed for plate specimens⁵. Representative data for symmetrical minor B-H loops for as-received VVER440 and VVER1000 samples are shown in Figs. 1(a) and 1(b), respectively. For each minor loop, we determined B-H parameters, i.e. maximum flux density, $B_{\rm a}^*$, and hysteresis loss, $W_{\rm F}^*$, and examined a power-law scaling relation between the two

¹⁾Department of Materials Science and Engineering, Faculty of Engineering, Iwate University, Ueda 4-3-5, Morioka 020-8551, Japan

²⁾ Centre for Energy Research, Hungarian Academy of Sciences, Budapest, Hungary

³⁾ Wigner Research Centre for Physics, Hungarian Academy of Sciences, Budapest, Hungary

⁴⁾ Key Laboratory of Neutron Physics and Institute of Nuclear Physics and Chemistry, China Academy of Engineering Physics, Mianyang 621999, China

⁵⁾ Jülich Centre for Neutron Science (JCNS) at Heinz Maier-Leibnitz Zentrum (MLZ), Forschungszentrum Jülich GmbH, 85748 Garching, Germany

a) Electronic mail: koba@iwate-u.ac.jp

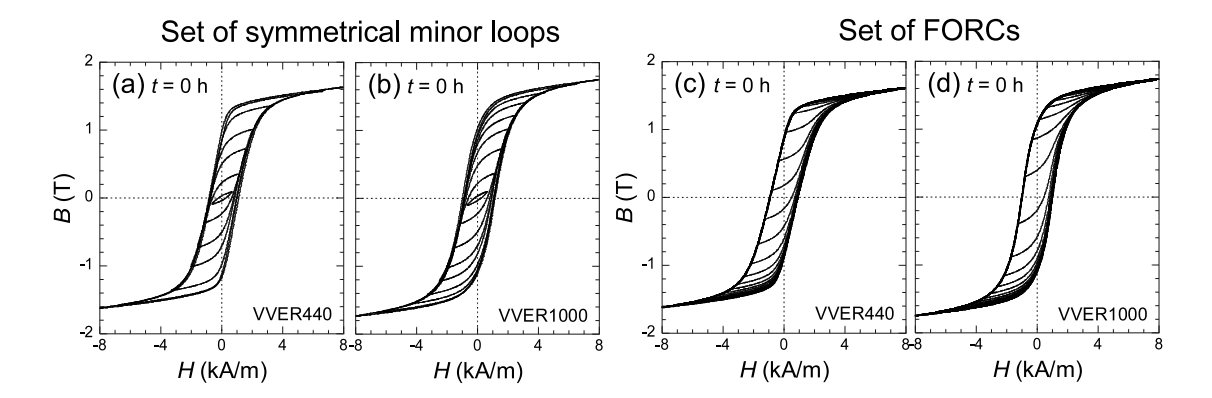


FIG. 1. A set of symmetrical minor B-H loops before aging for (a) VVER440 and (b) VVER1000. A set of FORCs before aging for (c) VVER440 and (d) VVER1000.

parameters, given by

$$W_{\rm F}^* = W_{\rm F}^0 \left(\frac{B_{\rm a}^*}{B_{\rm s}}\right)^{n_{\rm F}}.$$
 (1)

Here, $B_{\rm s}$ is a normalization constant which was set to 1.8 T. The relation was least-squares fitted using minor loops with $B_{\rm a}^*=0.25-1.1$ T, where irreversible motion of Bloch walls dominates the magnetization process, and an exponent of $n_{\rm F}=1.44\pm0.03$ was obtained, irrespective of the type of steels and aging time. We focused on the minor-loop coefficient, $W_{\rm F}^0$, being a sensitive indicator of defect density, and major-loop coercivity, $H_{\rm cm}$, obtained from a B-H loops with $H_{\rm a}=9$ kA/m.

FORCs were measured with a field sweep rate of 5 kA/m/s using the same fluxmeter as that for symmetrical minor-loop measurements. In this study, the measurements were performed for three aging time conditions; 0. 5, and 10 kh. Representative data of FORCs for asreceived VVER440 and VVER1000 samples are shown in Figs. 1(c) and 1(d), respectively. Starting at a reversal field, $H_{\rm r}$, on a descending branch of a major loop, the magnetic flux density, B, was measured with increasing magnetic field, H, until H reaches a positive saturation field of 9 kA/m. This process was repeated with changing $H_{\rm r}$ with a step of 450 A/m until $H_{\rm r}$ reaches a negative saturation field of -9 k/m, and totally 40 FORCs were taken for each sample. The observed B is a polynomial function of H and H_r . The FORC distribution, ρ , is the second derivative of B with respect to H and H_r , given by

$$\rho(H, H_{\rm r}) = -\partial^2 B / \partial H \partial H_{\rm r} \tag{2}$$

The calculated FORC distribution is plotted on a contour map with axes of interaction field, $H_{\rm u}$ and switching field, $H_{\rm c}$, which are given by $H_{\rm u}=(H+H_{\rm r})/2$ and $H_{\rm c}=(H-H_{\rm r})/2$, respectively. The switching field distribution, $\rho(H_{\rm c})$, given by $\rho(H_{\rm c},H_{\rm u})$ integrated over $H_{\rm u}$ was also calculated in order to investigate effects of domain wall pinning during thermal aging.

In order to investigate evolution of nanoscale features during thermal aging at 550°C, small-angle neutron scat-

tering (SANS) measurements were performed on both steels aged for 0, 5, and 10 kh. The experiments have been performed at the *YellowSubmarine* instrument at Budapest Neutron Centre, and on the KWS-1 instrument at Forschungszentrum Jülich¹⁰. The samples have been measured at ambient temperature and in a magnetic field of 2T perpendicular to the neutron beam, allowing to separate the magnetic and nuclear scattering.

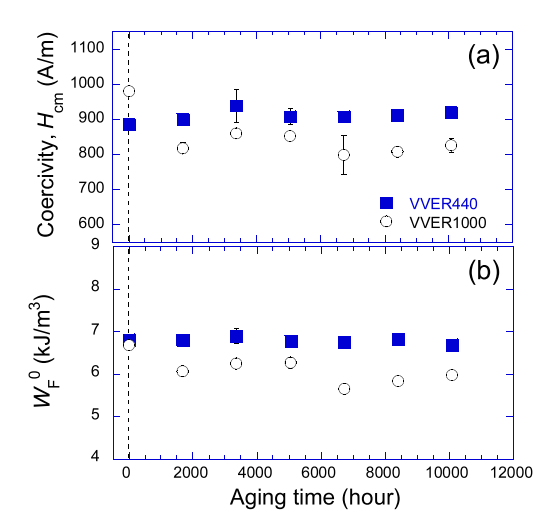


FIG. 2. (a) Major-loop coercivity, $H_{\rm cm}$ and (b) a minor-loop coefficient, $W_{\rm F}^0$, as a function of aging time for VVER440 and VVER1000. Error bars are primarily due to the sample dependence.

We also performed microhardness measurements and found that a change of microhardness due to thermal aging is within the experimental accuracy for both steels and is insensitive to thermal aging, as observed in a recent study¹².

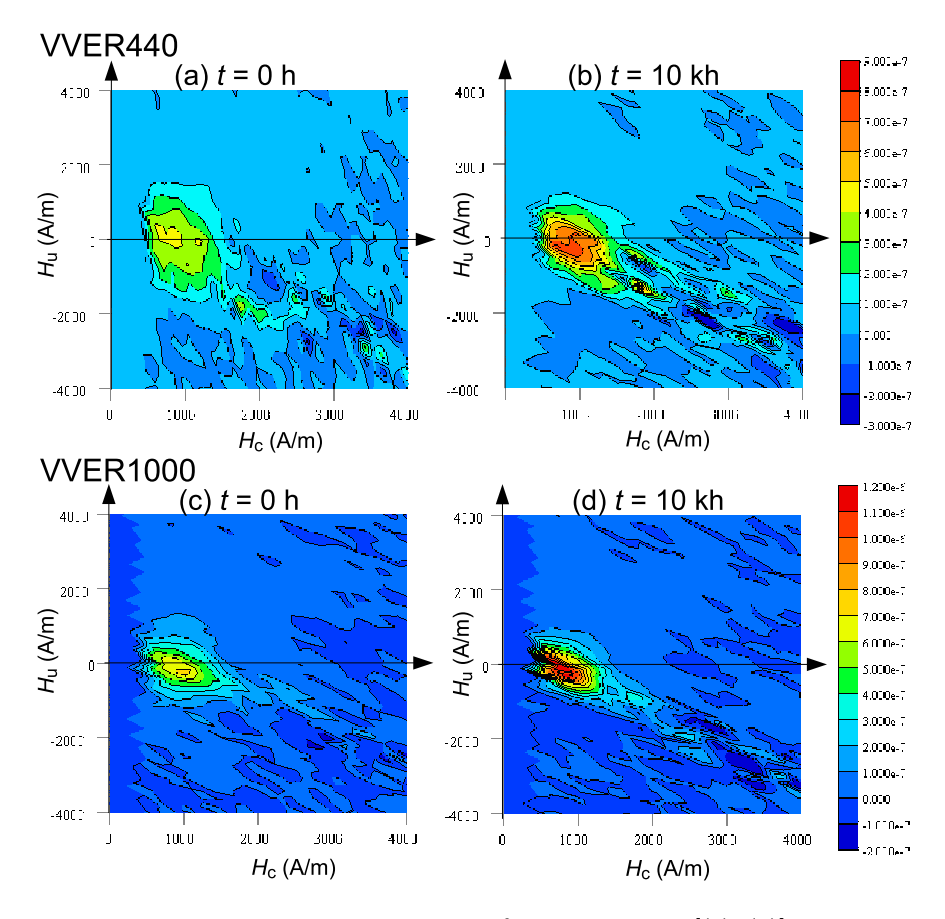


FIG. 3. FORC diagrams before and after aging at 550°C for VVER440 [(a), (b)] and VVER1000 [(c), (d)]

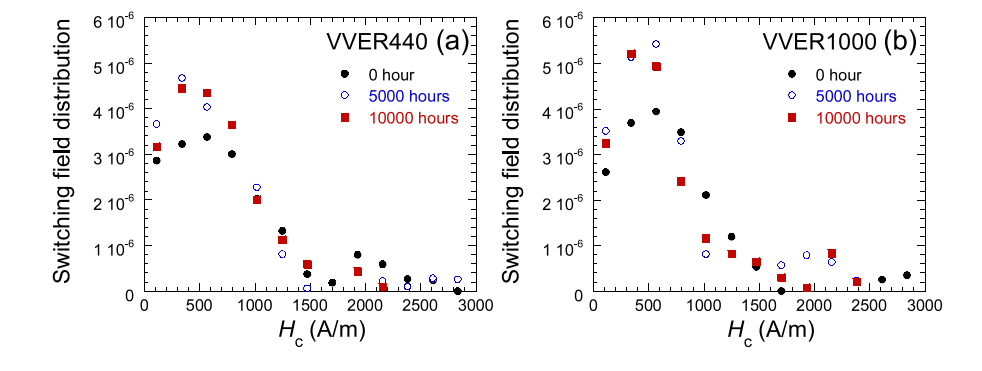


FIG. 4. Switching field distribution, $\rho(H_c)$, as a function of H_c before and after aging at 550°C for (a) VVER440 and (b) VVER1000.

III. RESULTS AND DISCUSSION

Figures 2(a) and 2(b) show $H_{\rm cm}$ and $W_{\rm F}^0$, as a function of aging time, respectively. While both $H_{\rm cm}$ and $W_{\rm F}^0$ are very weakly dependent on aging time for VVER440, those for VVER1000 with high-Ni content slightly decrease with aging time. Both of $H_{\rm cm}$ and $W_{\rm F}^0$ exhibit a similar aging dependence to each other and their decrease after aging up to 10 kh for VVER1000 is $\sim 15\%$ and 10% of as-received sample, respectively.

In Figs. 3(a)-3(d), FORC diagrams for VVER440 and 1000 before and after aging up to 10 kh are shown. For all the diagrams, the peaks are located at $H_{\rm u} \sim 0$, and $H_{\rm c}$, which corresponds to the major-loop coercivity $H_{\rm cm}$ shown in Fig. 2(a). We found that after aging up to 10 kh, FORC distributions for both VVER440 and VVER1000 become steep along both axes of interaction and switching fields and the peaks shift toward a lower $H_{\rm c}$. The peak shift of FORC distribution is reflected in the switching field distribution, $\rho(H_{\rm c})$, shown in Figs. 4(a) and 4(d), where the peak of $\rho(H_{\rm c})$ shifts

towards a lower H_c after aging for both VVER440 and VVER1000. The peak value of $\rho(H_c)$ is close to $H_{\rm cm}$, reflecting that the irreversible mechanism such as domain wall pinning dominates the magnetization process. The increase of the peak height is due to a narrowing of the FORC distribution along the $H_{\rm u}$ axis, which is related to a gradual transformation of a FORC into an ideal square hysteron¹¹. The observed FORC results are qualitatively consistent with the results of symmetrical minor loops.

Under irradiation, various types of lattice defects such as precipitates of a few nanometer size, carbides of a few tens nanometer size, dislocation loops, are formed. In particular, the volume fraction of precipitates after irradiation was found to be much higher for VVER1000 with high-Ni content². Although such formation is generally accelerated under irradiation due to irradiationinduced diffusion, nanoscale defects form also during thermal aging and their density would become high at higher aging temperatures. To investigate the structural changes on nanometer length scale during thermal aging, we performed SANS measurements for VVER440 and VVER1000 samples aged at 550°C. The experimental magnetic and nuclear scattering curves obtained before and after aging are almost identical, showing that there are no detectable changes for the amount of precipitates of sizes between 1 and 100 nm for both VVER440 and VVER1000 aged up to 10 kh^{13} .

According to an earlier theory for micromagnetism¹⁴. the arrangement of magnetization is determined so as to minimize magnetic Gibbs free energy consisting of exchange energy, magnetocrystalline anisotropy energy, magnetostatic energy, and magnetoelastic energy. In ferromagnetic steels including lattice defects, the Gibbs free energy is lowered when domain walls are located at lattice defects and the defects act as obstacles to the domain wall motion. Therefore, it is expected that steels with high defect density have high value of $H_{\rm cm}$, $W_{\rm E}^0$, as well as FORC distribution whose peak is located at a high value of H_c . However, the observed results showed that thermal aging at 550°C leads to a magnetic softening behavior; a decrease of $H_{\rm cm}$ and $W_{\rm F}^0$, and a peak shift of FORC distribution towards a lower H_c for both VVER440 and VVER1000 steels. The decrease of $H_{\rm cm}$ and $W_{\rm E}^0$ was large for VVER1000 with high-Ni content.

Impurity atoms dissolved in a Fe matrix cause a lattice strain around them and also act as a pinning center to domain walls¹⁴. In particular, Ni atom has a strong pinning effect and steels with a larger Ni content give higher $W_{\rm F}^{0.15}$. Considering that the precipitation during thermal aging is expected to be promoted by Ni¹⁶ and that there is no significant development of nanoscale precipitates (> 1 nm) during the aging as revealed by our SANS experiments, a decrease of lattice strain in the matrix, associated with the diffusion of Ni atoms to form precipitates, may dominate the observed magnetic behavior. Dissolved atoms including Ni may form precipitates during thermal aging, but their size would be very small (

<1 nm) and an effect of domain wall pinning at precipitates, which contributes to a magnetic hardening, would be negligibly small for VVER440 and VVER1000. A further study to directly observe such very small nanoscale features with atom probe tomography is planned.

IV. CONCLUSION

Effects of long-term thermal aging at 550° C up to \sim 10000 h for VVER440 and high-Ni VVER1000 pressure vessel steels were systematically investigated with three magnetic hysteresis methods using major-loop coercivity, hysteresis scaling of minor loops, and FORC distribution. We observed a decrease of major-loop coercivity and minor-loop coefficient of the scaling, as well as a peak shift of FORC distribution towards the lower coercivity axis. The magnetic results combined with SANS results suggest that a relaxation of lattice strain in the matrix, possibly associated with diffusion of Ni atoms, may dominate the development of magnetic properties during aging at 550° C.

ACKNOWLEDGMENT

This work was supported by Grant-in-Aid for Scientific Research (B) (Grant No. 25289346) from JSPS, Japan.

- ¹G.R. Odette, G.E. Lucas, Radiat. Eff. Def. Solids **144** (1998) 189.
- ² J. Bohmert, H.W. Viehrig, A. Ulbricht, J. Nucl. Mater. **297** (2001) 251.
- ³S. Kobayashi, F. Gillemot, A. Horváth, R. Székely, M. Horváth, Phil. Mag. **92** (2012) 3813.
- ⁴S. Kobayashi, F. Gillemot, A. Horváth, R. Székely, J. Nucl. Mater. **421** (2012) 112.
- ⁵S. Kobayashi, T. Yamamoto, D. Klingensmith, G. R. Odette, H. Kikuchi, Y. Kamada, J. Nucl. Mater. **422** (2012) 158.
- ⁶S. Takahashi, S. Kobayashi, H. Kikuchi, and Y. Kamada, J. Appl. Phys. **100** (2006) 113908.
- ⁷S. Kobayashi, S. Takahashi, T. Shishido, Y. Kamada, and H. Kikuchi, J. Appl. Phys. **107** (2010) 023908.
- ⁸C.R. Pike, A.P. Roberts, K.L. Verosub, J. Appl. Phys. **85** (1999) 6660.
- ⁹C.H. Henager Jr. J.S. McCoy, P. Ramuhalli, D.J. Edwards, S. Hu, Y. Li, Acta Materialia 61 (2013) 3285.
- ¹⁰ A.V. Feoktystov, H. Frielinghaus, Z. Di, S. Jaksch, V. Pipich, M.-S. Appavou, E. Babcock, R. Hanslik, R. Engels, G. Kemmerling, H. Kleines, A. Ioffe, D. Richter, and T. Brückel J. Appl. Cryst. 48 (2015) 61.
- ¹¹Y. Cao, K. Xu, W. Jiang, T. Droubay, P. Ramuhalli, D. Edwards, B.R. Johnson, J. McCoy, J. Mag. Mag. Mater. 395 (2015) 361.
- ¹²B. Gurovich, E. Kuleshova, Ya. Shtrombakh, S. Fedotova, D. Maltsev, A. Frolov, O. Zabusov, D. Erak, D. Zhurko, J. Nucl. Mater. 456 (2015) 23.
- ¹³The detailed SANS results will be given and discussed elsewhere.
 ¹⁴H. Kronmüler and M. FJähnle,
 MicromagnetismandtheMicrostructureofFerromagneticSolids,
 (Cambridge University, Cambridge, 2003).
- ¹⁵S. Kobayashi, H. Kikuchi, S. Takahashi, K. Chiba, Y. Kamada, K. Ara, Philos. Mag. 87 (2007) 4047.
- ¹⁶G.R. Odette, G.E. Lucas, D. Klingensmith, ASTM STP **1325** (1999) 88.